Water Research 191 (2021) 116792

Contents lists available at ScienceDirect

Water Research

journal homepage: www.elsevier.com/locate/watres

Effects of natural vegetation restoration on dissolved organic matter (DOM) biodegradability and its temperature sensitivity

Hongfei Liu[a,b,c], Hongwei Xu[a,c], Yang Wu[a,c], Zemin Ai[a,c], Jiaoyang Zhang[a,c], Guobin Liu[a,c], Sha Xue[a,c,*]

[a] State Key Laboratory of Soil Erosion and Dryland Farming on the Loess Plateau, Northwest A&F University, Yangling 712100, PR China
[b] Department of Agroecology, University of Bayreuth, Bayreuth 95440, Germany
[c] Institute of Soil and Water Conservation, Chinese Academy of Sciences and Ministry Water Resources, Yangling 712100, PR China

ARTICLE INFO

Article history:
Received 7 June 2020
Revised 23 December 2020
Accepted 24 December 2020
Available online 27 December 2020

Keywords:
Temperature sensitivity
DOM biodegradation
Dissolved organic carbon
Dissolved organic nitrogen
Three-dimensional excitation-emission matrix (EEM) fluorescence spectroscopy
Secondary vegetation succession

ABSTRACT

Biodegradation of dissolved organic matter (DOM) plays a key role in regulating both production of greenhouse gases and accumulation and stabilisation of soil organic matter (SOM). However, the mechanisms by which natural vegetation restoration affects the extent, rate, and temperature sensitivity of DOM biodegradation are poorly understood. Elucidating these mechanisms is important for SOM management, especially in light of future climate warming scenarios. In this study, a laboratory DOM solution incubation experiment was conducted to comprehensively investigate the effects of temperature and natural vegetation restoration spanning a period of 160 y on DOM biodegradation in the Loess Plateau, China. The results indicated that dissolved organic C (DOC) biodegradation significantly decreased with vegetation restoration after an incubation period of 60 d. Further, biodegradation of dissolved organic N (DON) and dissolved organic P (DOP) significantly decreased after farmland abandonment. Specifically, the lowest values were observed in pioneer (*Populus davidiana*) and mingled (*Populus davidiana* and *Quercus liaotungensis*) forests. Generally, an increase in temperature significantly promoted the biodegradation of DOC, DON, and DOP by enhancing the microbial utilisation efficiencies of recalcitrant humic substrates (i.e., low-molecular-weight humic materials). Our results suggest that DOM biodegradability and its temperature sensitivity were regulated by DOM substrate quality (i.e, recalcitrant humic materials), and microbial properties (i.e., gram-negative bacterial and fungal PLFA, enzyme activities). Additionally, our results suggest that climax forest communities (*Quercus liaotungensis*) played a vital role in reducing DOC and DOP losses. This could be attributed to the low Q10 of the DOC and DOP biodegradation rates.

1. Introduction

Although dissolved organic matter (DOM) is a minor fraction of total organic matter in soils (<0.25%), it is the most mobile and actively cycling organic matter. Additionally, it plays a key role in carbon storage and cycling, provides plant-available nutrients, and serves as an energy source for microorganisms (Kalbitz et al., 2000; Marschner and Kalbitz, 2003; McDowell et al., 2006). Moreover, DOM biodegradation significantly affects the soil organic matter (SOM) dynamics in soils. Further, it regulates the production of greenhouse gases (i.e., CO_2, CH_4, and N_2O) by providing electrons and reducing the soil O_2 content required for methanogenesis and denitrification (Lu et al., 2000; McDowell et al., 2006). Finally, it helps indicate processes that control SOM accumulation and stabilisation (Kaiser and Kalbitz, 2012). Therefore, understanding the dynamics of DOM biodegradation is important for SOM management and global climate change mitigation.

Natural vegetation restoration without anthropic interference is considered as an efficient measure for recovering both soil fertility and ecosystems with degraded soils (Prach and Walker, 2011). Revegetation significantly affects the DOM dynamics by altering the input of organic matter and influencing the rates, extent, and pathways of microbial degradation (Kalbitz et al., 2000; Liu et al., 2019). Specifically, DOM biodegradation is affected by intrinsic DOM characteristics (e.g., chemical structures of DOM compounds) and soil

Abbreviations: AMF, arbuscular mycorrhizal fungi; AP, Alkaline phosphatase; BG, β-glucosidase; DOM, dissolved organic matter; SOM, soil organic matter; DOC, dissolved organic carbon; DON, dissolved organic nitrogen; DOP, dissolved organic phosphorus; EEM, three-dimensional excitation-emission matrix; MBC, microbial biomass carbon; MBN, microbial biomass nitrogen; MBP, microbial biomass phosphorus; NAG, N-acetyl-β-glucosaminidases; PLFA, phospholipid fatty acid; Q10, temperature sensitivity; SEM, structural equation model.

* Corresponding author at: No. 26 Xinong Road, Yangling 712100, Shaanxi, China.
E-mail address: xuesha100@163.com (S. Xue).

https://doi.org/10.1016/j.watres.2020.116792
0043-1354/

factors (e.g., nutrient availability, microbial community structures, and microbial enzyme activities) (Marschner and Kalbitz, 2003). The conversion of sloped croplands to grasslands, shrublands, and woodlands has been shown to significantly increase the concentrations of dissolved organic C (DOC), dissolved organic N (DON), and recalcitrant substances (e.g., humic-like materials and fulvic acid) in DOM solutions and decrease DOC biodegradation in the Loess Plateau, China (Huang et al., 2015; Kalbitz et al., 2003a; Liu et al. 2019). Moreover, the succession rate of fungi has been shown to be significantly higher than that of bacteria in the Ziwuling forest region of Loess Plateau, China. Further, the relative abundances of microbial genes responsible for C and N cycling have been shown to decrease and increase with successional stages, respectively (Wang et al., 2019; Zhong et al. 2018). However, the effects of natural vegetation restoration on DOM biodegradation are poorly understood. Further, the mechanisms underlying DOM biodegradability are largely unknown.

Previous studies have concluded that microbial decomposition of soil organic matter and enzyme activities associated with soil C, N, and P cycling increased with increasing temperature (A'Bear et al., 2014; German et al., 2012; Min et al., 2019; Nazaries et al., 2015; Pang et al., 2015). Ylla et al. (2012) reported that labile organic matter (OM) was rapidly cycled irrespective of the temperature while microbial degradation of recalcitrant substances increased with increasing temperatures. Recalcitrant organic carbon (OC) fractions comprise more biochemically complex compounds than labile OC fractions; therefore, the decomposition of recalcitrant substrates requires greater activation energy (von Lützow and Kögel-Knabner, 2009). The 'carbon quality temperature' hypothesis states that temperature sensitivity increases with the increasing biochemical recalcitrance of soil organic matter (Davidson et al., 2006). Specifically, the Arrhenius equation dictates high temperature sensitivities for OC decomposition reactions occurring at high activation energies (Conant et al., 2011). Mao and Li (2018) concluded that the 'carbon quality temperature' hypothesis is applicable to DOC biodegradation. Further, DOC quality and pH are powerful predictors of the temperature sensitivity of biodegradable DOC in subtropical rivers. It has been reported that the temperature sensitivity of SOM decomposition is generally affected by substrate quality (i.e., soil C to N ratio, soil lignin and fatty acid content, and soil pH) and microbial properties (i.e., gram-negative bacterial PLFA, fungal PLFA, and fungi to bacteria ratio) (Liu et al., 2017a; Ma et al., 2019; Wang et al., 2018). Additionally, the 'carbon quality temperature' hypothesis is applicable to N mineralisation because its activation energy is strongly correlated with substrate quality (Miller and Geisseler, 2018; Schutt et al., 2014). Previous studies have reported that the temperature sensitivity of N mineralisation is affected by soil total nitrogen, soil C to N ratio, and soil pH (Liu et al., 2016; Liu et al., 2017b; Miller and Geisseler, 2018). Although several studies have focused on mechanisms regulating the temperature sensitivity of SOM decomposition, key factors regulating the temperature sensitivity of DOM biodegradation are largely unknown. Further, the mechanism by which natural vegetation restoration affects the temperature sensitivity of DOM biodegradation is poorly understood.

This study selected vegetation converted from adjacent farmlands with ages of 30, 60, 100, 130, and 160 years. This long-term and well-dated vegetation restoration chronosequence allowed comprehensive investigation of mechanisms by which natural vegetation restoration and temperature regulated DOM biodegradation in the Ziwuling forest region of the Loess Plateau, China. The DOM composition was investigated using three-dimensional excitation-emission matrix (EEM) fluorescence spectroscopy, which is a reagent-free, rapid, sensitive, and selective technique for fingerprinting organic matter in terrestrial ecosystems (Chen et al., 2003). This study aimed to elucidate the effects of natural vegetation restoration and temperature on DOM biodegradation. Further, the key factors driving DOM biodegradability were identified. Finally, the roles of substance quality and microbial properties in regulating the temperature sensitivity of DOM biodegradation were elucidated. We hypothesised that (1) DOM biodegradation significantly decreases after farmland abandonment. Further, variations in the biodegradation of DOC, DON, and dissolved organic P (DOP) could be attributed to mineralogical differences and different driving forces; (2) An increase in temperature significantly promotes DOM biodegradation by enhancing the decomposition of chemically recalcitrant substances; (3) Natural vegetation restoration significantly decreases the Q10 of DOM biodegradation, especially at the forest stage. This could be attributed to increased labile organic matter in DOM solutions and decreased Q10 of enzyme activities (resulting from altered microbial communities).

2. Methods

2.1. Study sites and soil sampling

The study sites were established on the Lianjiabian Forest Farm (35°03′–36°37′N, 108°10′–109°18′E, 1211–1453 m a.s.l.) in Heshui County, Ganshu Province, China (Fig S1). The Lianjiabian Forest Farm is located in the hinterland of the Ziwuling forest region of the Chinese Loess Plateau and covers a total area of 23,000 km^2. The study area is characterised by mid-temperate continental monsoon climate with a mean annual temperature of 10 °C and an average annual rainfall of 587 mm. This area has landforms typical of hilly-gully loess topography. The soils of this region developed from primary and secondary loess parent materials and are classified as Inceptisols (USDA Soil Taxonomical System) or loesses. The soils are evenly distributed above red earth (comprising calcareous cinnamon soils) at depths ranging from 50 to 130 m. The soil pH ranges from 7.92 to 8.31. Species-rich uniform forests cover this area, and the canopy density ranges from 80 to 95%.

According to previous studies, local inhabitants emigrated from the Ziwuling forest region due a national conflict (1842–1866). The subsequent secondary succession allowed natural regeneration of forests in the abandoned croplands. In particular, the complete sequence of natural vegetation succession following farmland abandonment can be observed in the study area. Chen (1954) investigated vegetation recovery in the Ziwuling forest region and reported that *P. davidiana* constituted 70% of the vegetation cover after ~100 years. Zou et al. (2002) investigated vegetation succession in this region at three temporal points (1962, 1982, and 2000) and concluded that *P. davidiana* forests had been replaced by *Q. liaotungensis* forests after ~50 years. The ages of herbaceous and shrub communities (<60 years of succession) were verified by consultations with local elders and by assessing land contracts between farmers and the government. The ages of forest communities with >60 years of recovery were determined by evaluating tree rings and examining relevant written sources. Five vegetation succession stages were selected as experimental sites: (1) grassland (~30 years, S30); (2) shrubland (~60 years, S60); (3) pioneer forest (~100 years, S100); (4) mingled forest (~130 years, S130); (5) climax forest (~160 years, S160). The dominant plant species for each vegetation succession stage is listed in Table S1. Notably, maize (*Zea mays* L.) was the only crop cultivated in the study area. Therefore, a maize farm with more than 200 years of cultivation history was selected as the reference (0 year). The aboveground biomasses of crops were harvested annually. Further, chemical fertilisers were applied annually, although the rate of application varied across the years. Study sites indicated similar elevations, gradients, and slopes and had been previously farmed in similar manners (Zhong et al., 2018). The detailed geographical and vegetation characteristics of

the study sites are presented in Table S1. Additionally, the soil chemical properties are listed in Table S2.

In this study, four sites each were established (at distances ranging from 0.3 to 1 km) for the restoration stages in August 2017. Further, a plot (20 × 20 m) was established at each site. Soil samples were collected from the top 20 cm using a stainless-steel corer (diameter: 5 cm) after removing the litter horizons. All sampling points were free of lichens, biological crusts, and any other vegetation within a radius of 0.75 m. Twenty soil cores were randomly collected along an S-shaped pattern from each plot. A total of 24 samples (6 sites × 4 replicate plots per site) were collected. All samples were sieved through a 2-mm screen to remove roots and other debris. One subsample was stored at 4 °C for subsequent use in the incubation experiment, and another subsample was air-dried for physicochemical analysis.

2.2. Preparation of DOM solutions and inocula

A DOM solution was prepared for each sample (Kalbitz et al., 2003b) with a dry soil to water ratio of 1:4 (w/w). All extracts were centrifuged at 3000 × g for 10 min and filtered through pre-washed 0.45 μm cellulose acetate filters (Schleicher and Schuell). The inocula were prepared by rewetting the soil samples to field capacity and incubating at 20 °C for 2 weeks to reactivate the microorganisms. Subsequently, 50 g of the incubated soil sample was shaken with 100 mL of 4 mM $CaCl_2$ for 30 min followed by filtration through 5 μm filters (Millipore, SMWP 4700).

2.3. Incubation experiments

The inocula were added to the respective DOM solutions at a ratio of 1:100 (Kalbitz et al., 2003b). Subsequently, the DOM solutions were stored in closed 2-L glass bottles with five glass-fibre filters to provide surface area for the establishment of biofilms (Kalbitz et al., 2003b). These solutions were incubated in the dark at 4, 20, and 35 °C for a duration of 60 days. Temperature is known to stimulate microbial activity within the physiological range of 0–35 °C (Paul and Clark, 1996). The solutions were gently shaken by hand for 2 min daily to mix the samples. Further, the incubation bottles were opened daily to aerate the DOM solutions. Subsamples were collected after 0, 1, 3, 7, 14, 22, 30, and 60 days. Each subsample was filtered through a 0.45 μm cellulose acetate membrane to remove both particulate matter and microorganisms. A total of 528 subsamples were collected and frozen prior to further laboratory analysis. The unfiltered subsamples were utilised for enzyme activity analysis.

2.4. Sample analysis

The DOC was determined using a TOC analyser (Liqui TOC II, Elementar, Germany). The total dissolved nitrogen (TDN) and total dissolved phosphorus (TDP) were estimated using the alkaline digestion/ultraviolet (UV) (Doyle et al., 2004) and ammonium molybdate (Galhardo and Masini, 2000) spectrophotometric methods, respectively. Concentrations of NH_4^+ and NO_3^- were measured by an AA3 continuous-flow autoanalyser (AutoAnalyzer3-aa3, Bran + Luebbe, Germany). The concentration of soluble reactive phosphorus (SRP) was determined using the phosphomolybdenum blue method (Murphy and Riley, 1962). The DON and DOP were calculated as TDN-($NH_4^+ + NO_3^-$) and TDP-SRP, respectively. If the DON or DOP is less than 20% of dissolved inorganic N or SRP, respectively, then the measurement errors might have negative influence on the precision of calculated results. In this study, DON or DOP were at least at the same order of magnitude compared to dissolved inorganic N or SRP, respectively, conforming that the calculation process of DON and DOP was valid. Analytical methods for determining other soil chemical properties and microbial parameters have been described in the materials and methods section of the supplementary material.

The EEM spectrograms of the subsamples were obtained using an LS-55 fluorescence spectrometer (PerKinElmer, USA). The slits for both excitation and emission were 5 nm with a scanning speed of 1200 nm min^{-1}. The EEMs were recorded at 2 nm intervals for excitation wavelengths (200–495 nm) and at 5 nm intervals for emission wavelengths (250–500 nm). The wavelength-dependent intensity of the light source and the light sensitivity of the detector were corrected before conducting the measurements. Correction factors supplied by the manufacturer were utilised to correct the excitation and emission intensities for instrument-specific biases.

The unfiltered subsamples were prepared for enzyme analysis. Specifically, the activities of β-glucosidase, N-acetyl-β-glucosaminidase, and alkaline phosphatase were measured using standard fluorimetric techniques described by DeForest (2009). Briefly, 50 μL (200 μM substrate) of the fluorimetric substrate solution and 150 μL of the subsample were mixed in a microplate and incubated for 2 h at the incubation temperature of the DOM solutions. Subsequently, 10 μL of 1.0 M NaOH was added to stop the reaction. Fluorescence was measured using a microplate fluorimeter (Molecular Devices SpectraMax M2 Multi-Mode Microplate Reader, USA) with 365 nm excitation and 450 nm emission filters. Each assay microplate contained two columns of blanks to correct background fluorescence in the substrates. The MUB-linked model substrates utilised for the enzyme analysis are presented in Table S3. The activities of β-glucosidase, N-acetyl-β-glucosaminidase, and alkaline phosphatase were expressed in μmol g^{-1} soil h^{-1}.

2.5. Parallel factor (PARAFAC) analysis

Each EEM was corrected for inner filtering effects by multiplying with a correction matrix (calculated for each wavelength pair from the sample absorbances). In this regard, the assumed excitation (Ex) and emission (Em) pathlengths were 0.5 cm in a 1-cm cuvette (Ohno, 2002). Data from the same vegetation communities were combined to avoid the admixing of various sources or environmental samples. The EEM spectrogram data were combined into six 3-dimensional arrays (88 samples × 51 excitations × 41 emissions). The Raman and Rayleigh scatter effects were removed from the data according to Liu et al. (2019). In order to identify the number of components in the model and to prove the validity of these components, four approaches including residual analysis, examine the spectral properties of each component, split half analysis, and random initialization was used.

Figure S2 presents the fluorescent components and the proportional distributions of soil DOM components. The Ex/Em wavelength pairs of component 1 (C1) were centred at 250/500 nm. This component was identified as a UVA humic-like component related to fulvic acid (Cory and McKnight, 2005; Stedmon and Markager, 2005). The Ex/Em wavelength pairs of component 2 (C2) were centred at 245/340 nm. This component was associated with protein-like materials (Murphy et al., 2006). A UVC humic-like fluorescent peak was observed for component 3 (C3) which was characterised by Ex/Em wavelength pairs centred at 239/480 nm. This component was associated with high-molecular-weight and aromatic humic materials (Cory and McKnight, 2005; Stedmon and Markager, 2005; Stedmon et al., 2003). A humic-like fluorescent peak was identified for component 4 (C4) which was characterised by Ex/Em wavelength pairs centred at 236/460 nm. This component was associated with low-molecular-weight materials and biological activity (Cory and McKnight, 2005; Murphy et al., 2006).

2.6. Data analyses

The least-square optimisation method was utilised to obtain a double-fitted exponential curve for elucidating the DOM biodegradation dynamics. Total DOM comprises both labile and stable DOM pools (Kalbitz et al., 2003b). This statistical analysis was performed utilising Auto2Fit 5.5 (7D-Soft High Technology Inc., Beijing, China).

Subsequently, DOM biodegradation was calculated as:

$$(\%\ of\ initial\ concentration) = (100-a)\times\left(1-e^{(-k2\times t)}\right) + a\times\left(1-e^{(-k1\times t)}\right)$$

where a is the proportion of labile DOM in total DOM (%), t is time (d), $k1$ is the biodegradation rate constraint of the labile DOM pool (d^{-1}), and $k2$ is the biodegradation rate constraint of the stable DOM pool (d^{-1}).

The half-lives of labile and stable DOM pools were calculated from loss-rate constraints as follows:

$$Half-life = \ln(2)\times k^{-1}$$

where K is the biodegradation rate constraint of the labile and stable DOM pools (d^{-1}).

The Q10 values of the DOM biodegradation rate and enzyme activity were calculated using the following equation:

$$Q10 = \left(\frac{k_{t2}}{k_{t1}}\right)^{[10/(t2-t1)]}$$

where K is the DOM biodegradation rate or enzyme activity at temperature t (°C).

Linear mixed models (LMMs) were used to analyse the individual and interactive effects of restoration stage, temperature, and incubation time on soil chemical properties, characteristics of DOM biodegradation, and enzyme activities. The models included 'restoration stage', 'temperature', and 'incubation time' as fixed effects and 'sampling site' as a random effect. All residues were checked for normality and homogeneity of variance. Further, Tukey's test ($P < 0.05$) was performed for multiple comparisons. A backward stepwise regression model was constructed to detect the effects of DOM composition, enzyme activities, and soil microbial properties on DOM biodegradation. The above mentioned statistical analyses were conducted using SPSS 21.0 (SPSS Inc., Chicago, IL, United States). Structural equation models (SEMs) were constructed to investigate the potential direct and indirect effects of DOM composition and microbial properties on the temperature sensitivities of DOM biodegradation and enzyme activities. The model was constructed and run in IBM SPSS + AMOS 21.0. The graphs were drawn using SigmaPlot 10.0 (Systat Software, San Jose, CA, United States). MATLAB 2014a (MathWorks Inc., USA) was used to analyse the EEM data. The fluorescence EEMs were analysed through PARAFAC modelling using the DOMFluor toolbox of MATLAB (Stedmon and Bro, 2008) following the procedures described by Stedmon and Bro (2008).

3. Results

3.1. DOM biodegradation at different successional stages

DOC biodegradation significantly decreased with natural vegetation restoration after the 60-day incubation period ($P < 0.05$, Fig. 1). The proportion of the labile DOC pool significantly decreased with succession, and the decrease rate was the highest during the first 30 years of vegetation restoration (Fig. 2 and Table 1). Farmland abandonment significantly decreased both DON biodegradation (after the 60-day incubation period) and the proportion of labile DON, which was the lowest at S30 and S100 followed by S60, S130, and S160 ($P < 0.05$, Fig. S3, Table S4). Additionally, NO_3^- concentrations in the DOM solutions slightly increased with the incubation duration and significantly decreased after farmland abandonment, especially within the first 100 years of vegetation restoration ($P < 0.05$, Fig. S3). However, NH_4^+ concentrations in the DOM solutions significantly increased within the first 100 years of vegetation restoration. Farmland abandonment significantly decreased both DOP biodegradation (after the 60-day incubation period) and the proportion of labile DOP ($P < 0.05$, Fig. S4, Table S5). Specifically, farmland abandonment decreased the biodegradation rates of both labile and stable DOPs (Table S5). Soluble reactive P (SRP) concentration in the DOM solution was low and remained relatively stable during the incubation period. Further, no significant differences in SRP concentrations were observed among the different stages of natural vegetation restoration.

3.2. DOM biodegradation at different temperatures

DOC biodegradation significantly increased with increasing temperature after the 60-day incubation period (Fig. 1). However, S160 indicated the highest DOC biodegradation at 20 °C (Fig. 1b). The biodegradation rate constant of labile DOC pool (K1) during 30 to 130 years of vegetation restoration was lowest at 35 °C, while highest biodegradation rate constant of stable DOC pool (K2) during the first 100 years of vegetation restoration was observed at 35 °C (Fig. 2). In contrast to the farmland, natural restoration significantly increased the Q10 of the DOC biodegradation rate between days 1 and 7 (Fig. 3a). Further, the Q10 was the highest at S130, followed by S100, S60, and S30, and the lowest at S160.

Elevated temperatures significantly promoted DON biodegradation after the 60-day incubation period (Fig. S3). However, the Q10 values of DON biodegradation rates at S30, S60, S100, and S130 were significantly lower than those of DOC biodegradation rates (Fig. 3b). Additionally, no significant differences in the Q10 values of the DON biodegradation rates were observed among the different vegetation restoration stages. Temperature exerted a negligible effect on the NO_3^- dynamics during the incubation period ($P > 0.05$). However, NH_4^+ concentrations in the DOM solutions were the lowest at 20 °C (Fig. S3). DOP biodegradation significantly increased with increasing temperature after the 60-day incubation period (Fig. S4). In contrast to the farmland, vegetation restoration significantly increased the Q10 of the DOP biodegradation rate between days 1 and 7. Further, the Q10 was the highest at S100 and S130, followed by S30 and S60, and the lowest at S160 (Fig. 3c). The SRP concentrations in the DOM solutions were the lowest at 4 °C (Fig. S4).

3.3. Changes in DOM composition during incubation

Natural vegetation restoration significantly affected the initial DOM composition and its dynamics during the incubation period ($P < 0.05$, Fig. 4). The initial concentrations of C1, C2, and C3 in DOM solutions from S130 and of C4 in DOM solutions from S30 and S130 were significantly higher than those from S0. However, the initial concentrations of C1 and C2 in DOM solutions from S60, S100, and S160 and of C3 in DOM solutions from S100 were significantly lower than those from S0 (Fig. 4). Notably, the effects of temperature on DOM composition varied with the different vegetation restoration stages. Specifically, elevated temperatures significantly increased the concentrations of C1 from S0 and S30 and of C2, C3, and C4 from S30. However, elevated temperatures significantly decreased the concentrations of C1 and C2 from S160 and of C3 and C4 from S130 and S160. Additionally, the concentrations of C1, C2, and C4 from S60 and S100 were the lowest at 20 °C and the highest at 35 °C.

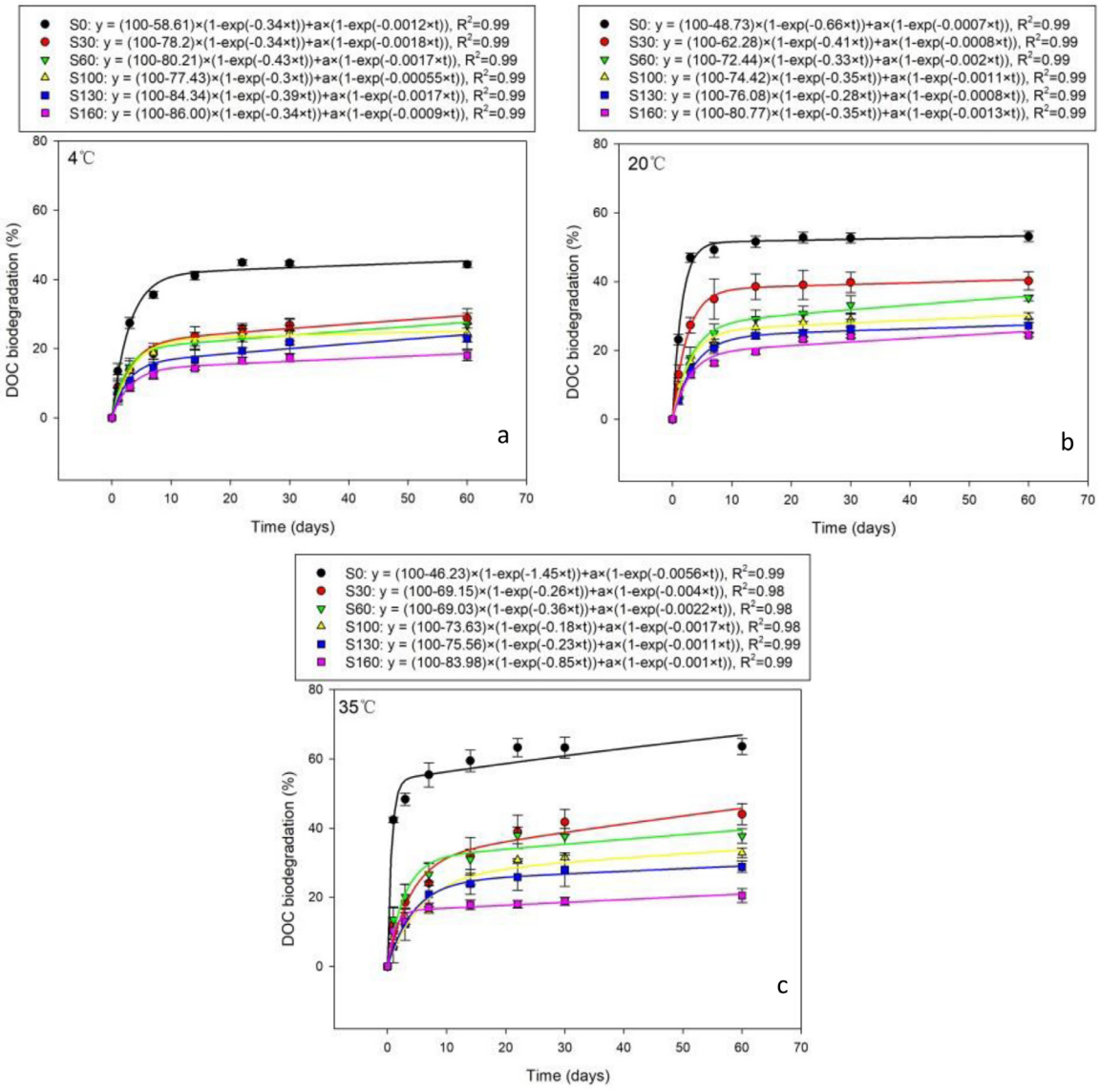

Fig. 1. Dynamics of DOC biodegradation from different successional stages during 60-day incubation at 4 °C (a), 20 °C (b), and 35 °C (c). Error bars represent one standard deviation ($n = 4$).

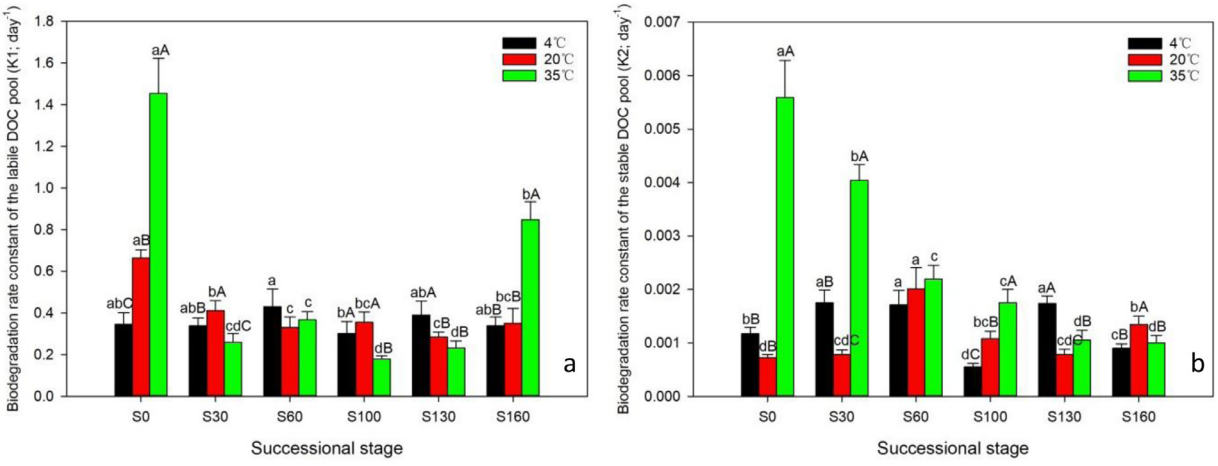

Fig. 2. Effect of the natural vegetation restoration and the temperature on the biodegradation rate constant of the labile (a) and stable (b) DOC pool. Error bars represent one standard deviation ($n = 4$). Different lowercase letters above the error bars indicate significant differences among different vegetation successional stage. Different capital letters above the error bars represent significant differences among temperature treatments within the same vegetation successional stage.

Table 1
Quantitative measures of the DOC biodegradation after 60 days incubation.

DOM solution	Biodegraded DOC % of total DOC	Labile DOC[a]	Stable DOC[b]	K1[c] (day^{-1})	K2[d] (day^{-1})	Half-life 1[e] (day)	Half-life 2[f] (year)	r^2
DOM solutions incubated at 4 °C								
S0	44.35	41.42	58.58	0.342	0.001	2.01	1.62	0.992
S30	28.75	21.79	78.21	0.338	0.002	2.05	1.09	0.991
S60	26.87	19.70	80.30	0.435	0.002	1.61	1.11	0.994
S100	24.50	22.55	77.45	0.298	0.001	2.30	3.45	0.991
S130	22.88	15.52	84.48	0.389	0.002	1.78	1.09	0.988
S160	17.96	13.87	86.13	0.343	0.001	2.05	2.11	0.991
DOM solutions incubated at 20 °C								
S0	53.07	48.65	51.35	0.662	0.001	1.04	2.75	0.997
S30	40.18	37.76	62.24	0.413	0.001	1.69	2.43	0.999
S60	35.21	27.59	72.41	0.330	0.002	2.10	0.94	0.998
S100	29.59	25.52	74.48	0.358	0.001	1.95	1.76	0.995
S130	27.25	23.99	76.01	0.284	0.001	2.44	2.43	0.999
S160	24.41	19.22	80.78	0.350	0.001	1.98	1.42	0.987
DOM solutions incubated at 35 °C								
S0	63.64	53.77	46.23	1.455	0.006	0.48	0.34	0.989
S30	44.03	30.85	69.15	0.259	0.004	2.68	0.47	0.985
S60	37.74	30.97	69.03	0.363	0.002	1.91	0.87	0.982
S100	32.85	26.37	73.63	0.179	0.002	3.88	1.09	0.978
S130	28.85	24.44	75.56	0.232	0.001	2.99	1.81	0.998
S160	20.48	16.03	83.98	0.847	0.001	0.82	1.90	0.990

r^2: *r*-square (coefficient of determination) of the double exponential model.
a: rapidly biodegradable DOC.
b: slowly biodegradable DOC.
c: biodegradation rate constant of the labile DOC pool.
d: biodegradation rate constant of the stable DOC pool.
e: half-life of the labile pool.
f: half-life of the stable pool.

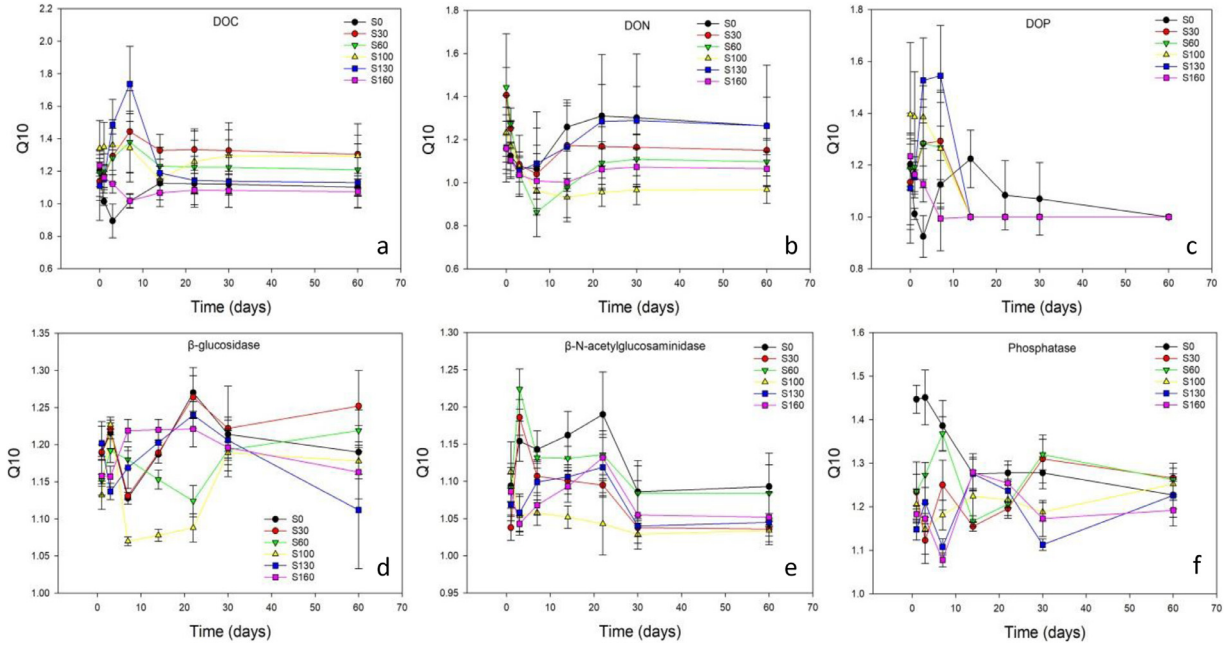

Fig. 3. Dynamics of Q10 values of DOC (a), DON (b) and DOP (c) biodegradation from different successional stages during 60-day incubation. Dynamics of Q10 values of β-glucosidase (d), β-N-acetylglucosaminidase (e) and phosphatase (f) biodegradation from different successional stages during 60-day incubation.Error bars represent one standard deviation ($n = 4$).

3.4. Changes in enzyme activities during incubation

Natural vegetation restoration and temperature significantly affected the enzyme activities during the incubation period ($P < 0.05$, Fig. 5). The activities of BG and AP were the highest at S100, followed by S60 and S160. Further, no significant differences were observed between S0, S30, and S130. The NAG activities were the highest at S100 and S160, followed by S130. However, no significant difference was observed for the first 60 years of natural vegetation restoration. Additionally, the activities of BG, NAG, and AP significantly increased with increasing temperature. The Q10 of BG was the highest at S30, followed by S0, S160, S130, and S60,

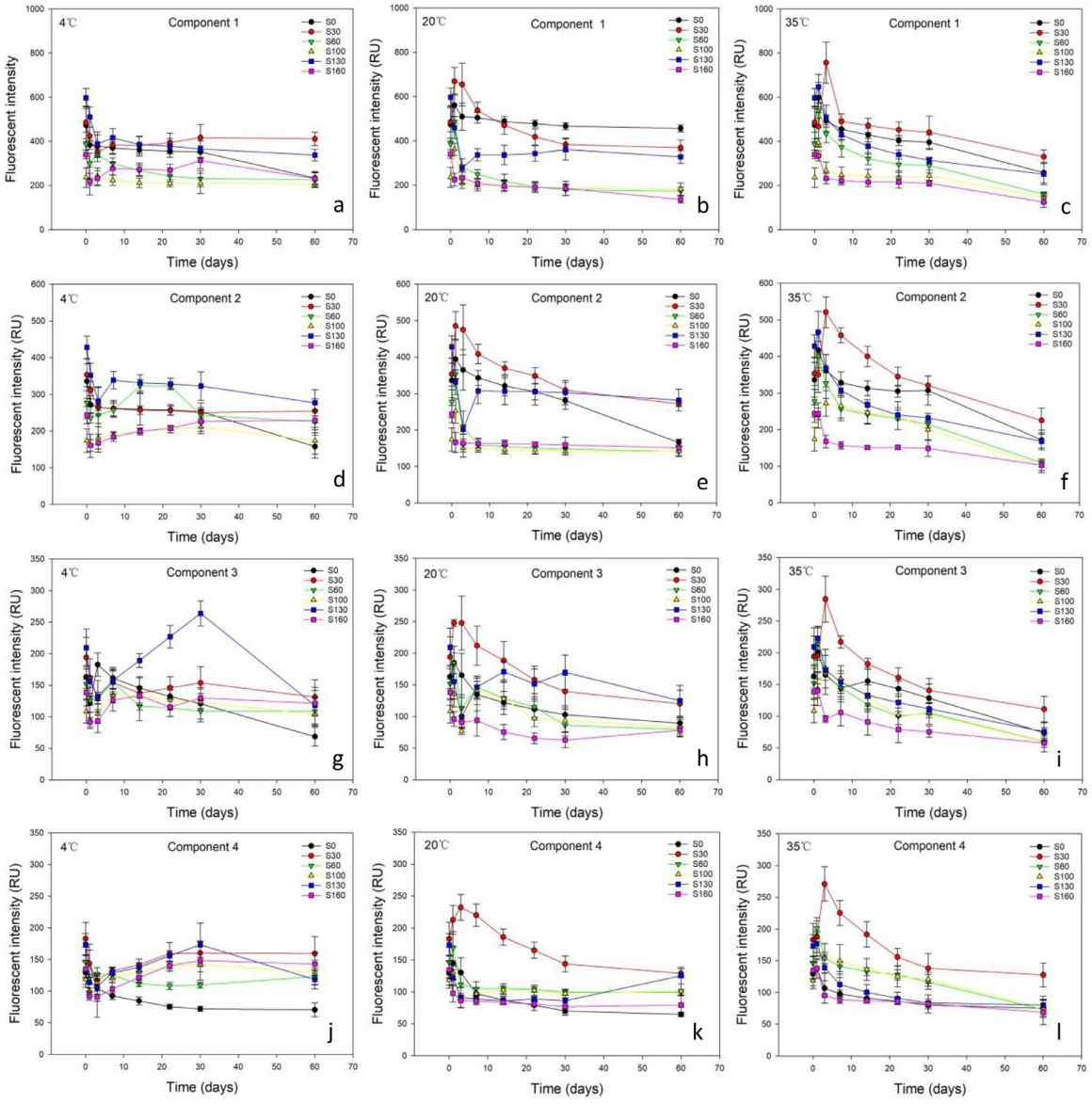

Fig. 4. Dynamics of Fmax values of the four components identified by PARAFAC in DOM solutions from different successional stages during incubation at different temperatures. Error bars represent standard deviation ($n = 4$).

and the lowest at S100 (Fig. 3d). The Q10 of NAG was the highest at S0 and S60, followed by S30, S130, and S160, and the lowest at S100 (Fig. 3e). Finally, the Q10 of AP was the highest at S0, followed by S60, and the lowest at S30, S100, S130, and S160 (Fig. 3f).

3.5. Factors affecting DOM biodegradation

The backward stepwise regression model indicated that fungal PLFA, AMF, and the fungi to bacteria ratio significantly affected DOC biodegradation at 4 °C while C3 and C4 exerted significant effects at 20 and 35 °C (Table 3). BG activity significantly affected the DOC biodegradation rate at 4 and 20 °C (Table 2). Microbial biomass carbon (MBC) affected both labile and stable DOC biodegradation rates at 4 °C (Table 3). Further, the fungi to bacteria ratio affected the labile DOC biodegradation rate at 4 °C. Both labile and stable DOC biodegradation rates were affected by fungal PLFA at 20 °C. Additionally, microbial biomass phosphorus (MBP) and AMF positively affected the labile (at 30 °C) and stable DOC biodegradation rates, respectively.

The backward stepwise regression model also indicated that C1, C4, gram-positive and gram-negative bacterial PLFA, AMF, and the fungi to bacteria ratio significantly affected DON biodegradation (Table 3). Further, BG, NAG, AP, and C1 significantly affected the DON biodegradation rate during incubation (Table 2). Additionally, C3 concentrations in the DOM solutions affected the DON biodegradation rate only at 4 °C (Table 3). Notably, C3, C4, gram-positive and gram-negative bacterial PLFA, MBP, and the fungi to bacteria ratio significantly affected DOP biodegradation (Table 3). Further, NAG, AP, and C1 significantly affected the DOP biodegradation rate during incubation (Table 2). Factors affecting DOP biodegradation shifted from C2, gram-negative bacterial PLFA, MBP, and the fungi to bacteria ratio at 4 °C to MBP at 20 °C, and microbial biomass nitrogen (MBN) at 35 °C (Table 3).

3.6. Factors affecting the temperature sensitivity of DOM biodegradation

The SEM 1 explained 60, 24, and 67% of the variance in the Q10 values of the DOC biodegradation rate, BG activity, and AP activity,

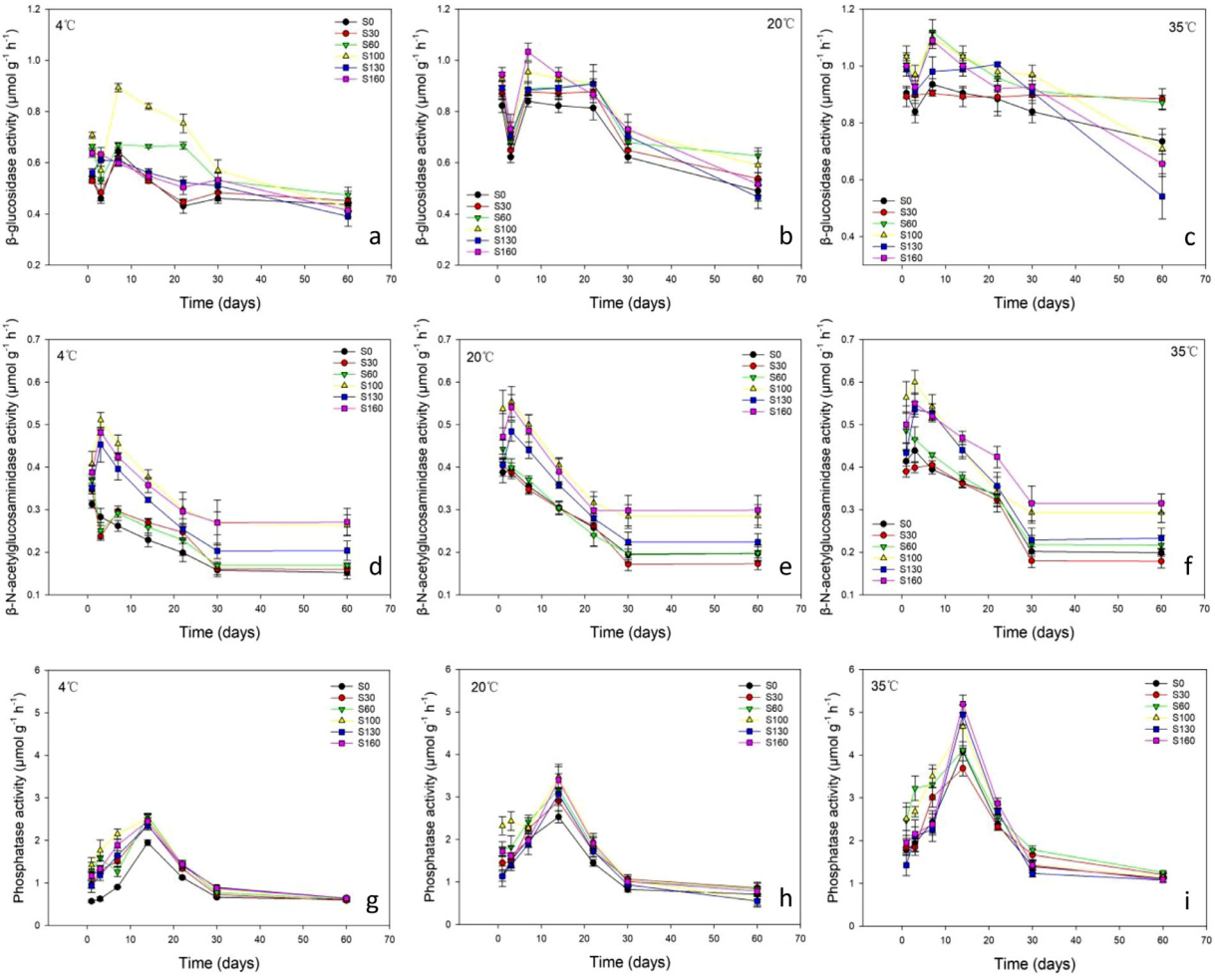

Fig. 5. Dynamics of enzyme activities in DOM solutions from different successional stages during incubation at different temperatures. Error bars represent standard deviation ($n = 4$).

Table 2
Summary of backward stepwise regression models to detect DOC biodegradation rate, DON biodegradation rate and DOP biodegradation rate as determined by enzyme activities and DOM composition.

	Equations	r^2	F	P	n
All temperature	$y1 = 1.553 \times 1 + 11.218 \times 2\text{-}1.044 \times 3 + 0.005 \times 4\text{-}0.009 \times 6 + 0.011 \times 7\text{-}3.670$	0.386	52.000	0.000**	504
	$y2 = 0.325 \times 1 + 3.945 \times 2\text{-}0.363 \times 3 + 0.003 \times 4\text{-}0.002 \times 6\text{-}1.121$	0.469	88.117	0.000**	504
	$y3 = 0.076 \times 2\text{-}0.007 \times 3 + 0.0000421 \times 4\text{-}0.02$	0.331	61.626	0.000**	504
Incubations at 4 °C	$y1 = 3.124 \times 1 + 8.466 \times 2\text{-}1.301 \times 3 + 0.008 \times 4\text{-}0.013 \times 6\text{-}2.305$	0.349	17.361	0.000**	168
	$y2 = 1.093 \times 1 + 3.287 \times 2\text{-}0.48 \times 3 + 0.003 \times 4\text{-}0.005 \times 6\text{-}1.083$	0.471	28.812	0.000**	168
	$y3 = 0.074 \times 2\text{-}0.011 \times 3 + 0.00004 \times 4\text{-}0.013$	0.227	16.097	0.000**	168
Incubations at 20 °C	$y1 = 5.408 \times 1 + 9.997 \times 2\text{-}1.433 \times 3 + 0.007 \times 4\text{-}0.008 \times 5 + 0.012 \times 7\text{-}5.833$	0.471	23.925	0.000**	168
	$y2 = 1.332 \times 1 + 3.827 \times 2\text{-}0.472 \times 3 + 0.002 \times 4\text{-}1.667$	0.496	40.102	0.000**	168
	$y3 = 0.036 \times 1 + 0.064 \times 2\text{-}0.01 \times 3 + 0.00004 \times 4\text{-}0.038$	0.418	29.032	0.000**	168
Incubations at 35 °C	$y1 = 11.599 \times 2\text{-}0.852 \times 3\text{-}0.015 \times 5 + 0.016 \times 7 + 0.011 \times 4\text{-}3.035$	0.475	29.273	0.000**	168
	$y2 = 3.668 \times 2\text{-}0.32 \times 3 + 0.003 \times 4\text{-}1.067$	0.492	52.930	0.000**	168
	$y3 = 0.072 \times 2\text{-}0.006 \times 3 + 0.00005 \times 4\text{-}0.019$	0.372	32.351	0.000**	168

$x1$, β-glucosidase activity; $x2$, β-N-acetylglucosaminidase activity; $x3$, phosphatase activity; $x4$, fluorescent component 1; $x5$, fluorescent component 2; $x6$, fluorescent component 3; $x7$, fluorescent component 4; $y1$, DOC mineralization rate; $y2$, DON mineralization rate; $y3$, DOP mineralization rate.

respectively (Fig. 6). The concentrations of C1 and C4 and the Q10 of BG and AP activities exerted direct negative effects on the Q10 of the DOC biodegradation rate while AMF exerted a direct positive effect. Notably, the Q10 values of BG and AP activities were determined by MBC, MBN, MBP, and fungal PLFA. Further, MBN exerted a significant negative effect on the Q10 of BG and AP activities, AMF, and fungal PLFA.

The SEM 2 explained 43, 70, and 53% of the variance in the Q10 values of the DON biodegradation rate, NAG activity, and AP activity, respectively (Fig. S5a). The Q10 of NAG and AP activities exerted direct positive effects on the Q10 of the DON biodegradation rate. Further, AMF and MBP exerted significant negative effects on the Q10 of NAG. Additionally, MBC exerted direct effects on AMF, MBP, and the Q10 of NAG and AP activities. The SEM 3 explained 47, 70, and 83% of the variance in the Q10 of the DOP biodegrada-

Table 3
Summary of backward stepwise regression models to detect 60-day biodegradation and half-lives of labile and stable pools of DOC, DON, DOP as determined by DOM composition and soil microbial properties.

	Equations	r^2	F	P	n
All temperature	$y1 = 0.001 \times 3\text{-}0.001 \times 4 + 0.028 \times 7\text{-}0.038 \times 8 + 0.309 \times 9\text{-}0.003 \times 10 + 0.274$	0.700	25.231	0.000**	72
	$y2 = -0.007 \times 4\text{-}0.005 \times 6 + 0.179 \times 8 + 2.357$	0.117	4.563	0.014*	72
	$y3 = -0.002 \times 1 + 0.006 \times 4 + 0.193 \times 8 + 1.046$	0.298	29.779	0.000**	72
	$y4 = 0.055 \times 1\text{-}0.169 \times 4 + 0.319 \times 5\text{-}0.179 \times 6\text{-}2.002 \times 8 + 19.201 \times 9 + 34.561$	0.517	11.579	0.000**	72
	$y5 = 0.002 \times 3\text{-}0.004 \times 4 + 0.002 \times 5\text{-}0.002 \times 6\text{-}0.002 \times 12 + 0.706$	0.395	8.628	0.000**	72
Incubations at 4 °C	$y1 = 0.027 \times 7\text{-}0.04 \times 8 + 0.355 \times 9\text{-}0.002 \times 12 + 0.112$	0.770	15.860	0.000**	24
	$y2 = -0.003 \times 1\text{-}0.014 \times 4 + 0.028 \times 5\text{-}0.021 \times 6 + 3.155 \times 9\text{-}0.002 \times 10 + 0.209 \times 7 + 2.677$	0.868	15.048	0.000**	24
	$y3 = -0.005 \times 3 + 0.007 \times 6\text{-}0.005 \times 10 + 0.012 \times 11 + 2.284$	0.567	6.223	0.000**	24
	$y4 = 0.053 \times 1\text{-}0.202 \times 4 + 0.427 \times 5\text{-}0.284 \times 6 + 19.237 \times 9\text{-}1.09 \times 8 + 33.166$	0.778	9.917	0.000**	24
	$y5 = 0.001 \times 2\text{-}0.004 \times 4 + 0.005 \times 5\text{-}0.004 \times 6 + 0.196 \times 9\text{-}0.003 \times 12 + 0.595$	0.727	7.560	0.000**	24
Incubations at 20 °C	$y1 = 0.001 \times 3\text{-}0.002 \times 4\text{-}0.004 \times 12 + 0.58$	0.864	42.338	0.000**	24
	$y2 = 0.016 \times 3\text{-}0.017 \times 4\text{-}0.01 \times 11 + 0.143 \times 7 + 1.974$	0.518	5.108	0.006**	24
	$y3 = 0.006 \times 7 + 0.003 \times 10{+}0.311$	0.639	18.579	0.000**	24
	$y4 = 0.054 \times 1\text{-}0.146 \times 4 + 0.253 \times 5\text{-}0.115 \times 6 + 19.268 \times 9\text{-}2.5 \times 8 + 33.49$	0.892	23.511	0.000**	24
	$y5 = -0.001 \times 4\text{-}0.002 \times 12 + 0.547$	0.383	6.509	0.006**	24
Incubations at 35 °C	$y1 = 0.001 \times 3\text{-}0.002 \times 4\text{-}0.005 \times 12 + 0.706$	0.864	42.338	0.000**	24
	$y2 = 0.007 \times 1\text{-}0.019 \times 3 + 0.015 \times 5\text{-}0.01 \times 6 + 0.021 \times 12 + \ + 0.388$	0.833	18.015	0.000**	24
	$y3 = -0.039 \times 1 + 0.044 \times 2 + 0.022 \times 3\text{-}0.023 \times 5 + 0.665 \times 8 + 0.173$	0.745	10.495	0.000**	24
	$y4 = 0.056 \times 1\text{-}0.16 \times 4 + 0.278 \times 5\text{-}0.139 \times 6\text{-}2.415 \times 8 + 19.098 \times 9 + 37.027$	0.904	26.720	0.000**	24
	$y5 = -0.001 \times 4\text{-}0.001 \times 11 + 0.638$	0.505	10.727	0.000**	24

$x1$, fluorescent component 1; $x2$, fluorescent component 2; $x3$, fluorescent component 3; $x4$, fluorescent component 4; $x5$, gram-positive bacteria; $x6$, gram-negative bacteria; $x7$, fungi; $x8$, AMF; $x9$, fungi to bacteria ratio; $x10$, microbial biomass carbon; $x11$, microbial biomass nitrogen; x12, microbial biomass phosphorus; $y1$, 60-day decomposition of DOC; $y2$, half-life of labile DOC; $y3$, half-life of stable DOC; $y4$, 60-day decomposition of DON; $y5$, 60-day decomposition of DOP.

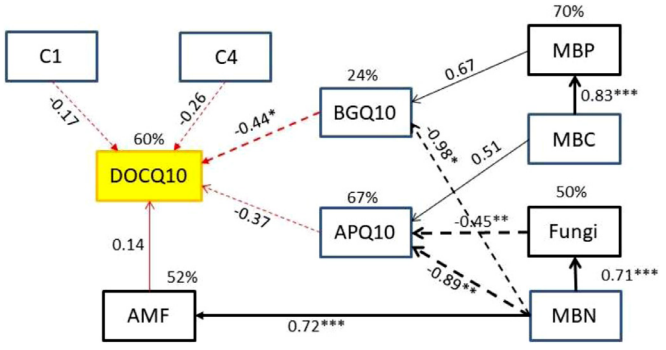

Fig. 6. Structural equation model of the effects of DOM composition, microbial properties, and temperature sensitivity (Q10) of enzyme activity on Q10 of DOC. Models a satisfactorily fitted to data based on $\chi 2$ and RMSEA analyses [model a: $\chi 2 = 32.002$, df = 26, $P = 0.193$, GFI = 0.928, RMSEA = 0.033]. Solid and dashed arrows represent the positive and negative effects in a fitted structural equation model, respectively. Widths of the arrows indicate the strength of the casual relationship (the standardized path coefficients on arrows). Variances explained by the model (R^2) are shown next to each endogenous variable.

tion rate, AP activity, and NAG activity, respectively (Fig. S5b). The Q10 of NAG and AP activities exerted direct negative effects on the Q10 of the DOP biodegradation rate, while C4 concentration exerted a direct positive effect. The Q10 of AP activity was negatively affected by fungal PLFA and MBN. Fungal PLFA exerted direct negative effects on the Q10 of NAG and AP activities and were directly and positively affected by MBC and MBN.

4. Discussion

4.1. Effects of natural vegetation restoration on DOM biodegradation

Previous studies conducted in the Ziwuling forest region indicated that both litter and soil organic carbon decomposition rate decreased during the succession from grasslands to climax forests, with the highest rate observed for grasslands (Deng et al., 2016; Zhong et al., 2018). In this study, consistent with our hypothesis 1, DOC biodegradation significantly decreased in response to natural vegetation restoration after the 60-day incubation period ($P < 0.05$, Fig. 1). This result is partly supported by a previous study conducted in the Loess Plateau which concluded that the conversion of sloped croplands to grasslands, shrublands, and woodlands significantly decreased DOC biodegradation (Liu et al., 2019). Further, it has been reported that arable lands and grasslands in northeastern Germany exhibit significantly high degradation of DOC in contrast to natural forests, which is consistent with our results (Kalbitz et al., 2003a). The backward stepwise regression analysis indicated that DOC biodegradation and its rate were affected by both DOM composition and microbial properties (Tables 2 and 3). DOC biodegradation was positively affected by the initial concentration of high-molecular-weight and aromatic humic component (C3), fungi, and the fungi to bacteria ratio after the 60-day incubation period, but negatively affected by the initial concentration of low-molecular-weight humic component (C4), AMF, and MBC. This could be attributed to the following: (1) C4 is more recalcitrant than C3 because humic acids with high molecular weights are readily degradable (Kisand et al., 2008); (2) The succession rate of fungi was significantly higher than that of bacteria in the Ziwuling forest region. Further, the relative abundances of C cycle genes decreased with the successional stages (Wang et al., 2019; Zhong et al., 2018). (3) Fungi exhibit a significant capacity for utilising recalcitrant soil organic matter by producing a wide range of extracellular enzymes that decompose recalcitrant structural compounds such as lignocelluloses and humus (Peay et al., 2008). Further, the fungi to bacteria ratio is significantly correlated with ecosystem processes such as decomposition and nutrient cycling (Goberna et al., 2012); (4) Although AMF generally lack saprotrophic capability, they can compete with saprotrophic microbes specific to OC degradation for N and P sources (Morrison et al., 2017; Teutscherova et al., 2019; Zhang et al., 2016). This could diminish the microbial DOC decomposition activity in N and P deficient soils. Therefore, the increased recalcitrant component of humic materials in DOM (Fig. 4) and AMF (Table S6) along with vegetation restoration exerted direct and indirect effects to inhibit DOC biodegradation. This is important for reducing the loss of bioavailable C in the Loess Plateau. Additionally, the DOC biodegradation rate during incubation was primarily affected by the enzyme ac-

tivities involved in C, N, and P cycling. Soil microbes preferentially use readily available substrates when available N is sufficient, while soil microbes decompose SOM for mining N when N is limiting (Blagodatskaya and Kuzyakov, 2008; Fontaine et al., 2003; Luo et al. 2016). Contrarily, C2 (a protein-like material highly related to biodegradable DOC) played a negligible role in regulating DOC biodegradation (Fellman et al., 2008).

Farmland abandonment significantly decreased DON biodegradation ($P < 0.05$, Fig. S3), which supported our hypothesis 1. Specifically, pioneer forests (~100 y) and grasslands (~30 y) indicated significantly lower DON biodegradation than shrubs (~60 y), mingled forests (~130 y), and climax forests (~160 y). Zhong et al. (2018) reported that S100 indicated the highest potential for ammonia and nitrate assimilation. Further, unlike C cycle genes, the relative abundances of N cycle genes increased from S30 to S100. The backward stepwise regression analysis indicated that fulvic acid played a key role in regulating DON biodegradation and its biodegradation rate (van Hees et al., 2005). Notably, fulvic acid is an important component of DOC which affects the biological availability of organic chemicals. Additionally, DON biodegradation was affected by bacteria, AMF, and the fungi to bacteria ratio. It has been reported that vegetation restoration resulted in the shift of bacterial communities from slow-growing oligotrophic groups (*Gemmatimonadetes* and *Chloroflexi*) to fast-growing copiotrophic groups (*Alpha-* and *Betaproteobacteria*) (Wang et al., 2019). The results of our study indicated that enzyme activities involved in C and P cycling affected DON biodegradation, which is partly supported by Schmidt et al. (2011), who reported that DON decomposition was driven by the microbial C demand. In agreement with Ghani et al. (2013), no decreases were observed in the concentrations of NO_3^- and NH_4^+ during incubation, thus conforming that DON was the most microbial preferred source of N.

Consistent with our hypothesis 1, farmland abandonment significantly decreased DOP biodegradation ($P < 0.05$, Fig. S4), with the lowest value observed for mingled forests (~130 y). This could be attributed to the decreased turnover rates of both labile and stable DOPs after vegetation restoration. DOP biodegradation was affected by gram-positive bacteria, MBP, and the fungi to bacteria ratio. Further, the DOP biodegradation rate was affected by enzyme activities involved in N and P cycling during incubation. In contrast to gram-negative bacteria, gram-positive bacteria are known to utilise a higher variety of substrates ranging from easily available to more complex compounds (Ali et al., 2015; Müller et al., 2016). The results of this study indicated that microbial phosphorus availability and microbial phosphorus assimilation ability played a significant role in regulating DOP biodegradation. Notably, N availability significantly increased within the first 130 y of vegetation restoration (Table S2). Consequently, N limitation for microbes was relieved while P limitation for microbes increased during the later stages of vegetation restoration (Ortiz-Álvarez et al., 2018; Schmidt et al., 2011; Zhong et al., 2018).

4.2. Effects of natural vegetation restoration on the temperature sensitivity of DOM biodegradation

Numerous studies have reported that an increase in temperature increases both microbial decomposition of soil organic matter and enzyme activities related to soil C, N, and P cycling (A'Bear et al., 2014; German et al., 2012; Liu et al., 2017a; Min et al., 2019; Nazaries et al., 2015; Pang et al., 2015). In the present study, an increase in temperature significantly increased DOC biodegradation (except at S160, which indicated the highest DOC biodegradation at 20 °C), which supported our hypothesis 2. The backward stepwise regression analysis indicated that DOC biodegradation at 4 °C was limited by microbial properties such as fungal PLFA, AMF PLFA, and the fungi to bacteria ratio. Contrarily, DOC biodegradation at 20 and 35 °C was limited by humic-like materials in the DOM solutions. The low concentrations of C3 and C4 at S160 restricted microbial degradation at high temperatures, thus resulting in low DOC biodegradation at 35 °C. The DOC biodegradation rate was affected by high-molecular-weight humic materials at 4 °C and low-molecular-weight humic materials at 20 and 35 °C. These results are in agreement with those of Allison et al. (2010) and Frey et al. (2013) and confirm that increasing temperatures promoted the microbial utilisation efficiency of more recalcitrant humic substrates (von Lützow and Kögel-Knabner, 2009). This could be attributed to the higher activation energy required for the decomposition of recalcitrant substrates. Notably, BG activity, which significantly increased with increasing temperature, did not limit the DOC biodegradation rate at 35 °C. Furthermore, the microbial utilisation efficiency of labile carbon (indicated by increased gram-negative bacterial PLFA and MBC) was an important factor that limited the DOC turnover rate at low temperatures. In contrast, recalcitrant C substrates (e.g., fulvic acid and aromatic humic-like materials) and microorganisms responsible for recalcitrant carbon decomposition (e.g., fungi and gram-positive bacteria) determined the turnover rates of both labile and stable DOCs with increasing temperature.

The temperature sensitivity (Q10) of the DOC biodegradation significantly increased over the first 130 years of vegetation restoration, but rapidly decreased between 130 y and 160 y, which partly supported our hypothesis 3. Specifically, the value at S160 was as low as that at S0 (Fig. 3). The 'carbon quality temperature' hypothesis states that temperature sensitivity increases with the biochemical recalcitrance of soil organic matter (Davidson et al., 2006). Previous studies have concluded that substrate quality (i.e., soil C:N ratio, soil lignin and fatty acid content, and soil pH) and microbial properties (i.e., gram-negative bacterial PLFA, fungal PLFA, fungi to bacteria ratio, and actinomycetes to bacteria ratio) affect the temperature sensitivity of SOM decomposition (Liu et al., 2017a; Ma et al., 2019; Wang et al., 2018). In this study, the results of SEM 1 highlighted that the temperature sensitivity of DOC biodegradation was directly affected by the initial concentrations of C1 and C4, the temperature sensitivity (Q10) of enzyme activities involved in C and P cycling, and AMF. A previous study concluded that AMF increased the decomposition of soil organic carbon in response to elevated CO_2 levels by stimulating (i.e., priming) the saprotrophs in soils (Cheng et al., 2012). Further, the study concluded that AMF-microbiome interactions via carbon and phosphorus exchange likely enhanced the mineralisation of organic P (Zhang et al., 2018, Zhang et al., 2016). Therefore, the temperature sensitivity of DOC biodegradation was affected by factors regulating C cycling (i.e., biochemical recalcitrant substances and Q10 of BG and AMF) and the factors related to P cycling (Q10 of AP and AMF). Significantly decreased initial concentrations of C1 and C4 from 130 to 160 y as well as decreased PLFA of gram-negative bacteria, fungi, and AMF from 100 to 160 y contributed to the low temperature sensitivity of DOC biodegradation at the climax forest stage.

As our hypothesis 2, an increase in temperature significantly promoted DON biodegradation after the 60-day incubation period (Fig. S3). Liu et al. (2016) reported a strong correlation between the activation energy of nitrogen mineralisation and the substrate quality index. Further, they highlighted the applicability of the carbon-quality temperature hypothesis to N mineralisation. In this study, concentrations of high-molecular-weight and aromatic humic materials (C3) negatively affected the DON biodegradation rate at 4 °C, but had a negligible effect on DON biodegradation rate at 20 and 35 °C, thus indicating that DON biodegradation at 4 °C was limited by microbial C degradation, and microbial C3 degradation promoted DON biodegradation with increasing temperature. However, the temperature sensitivity (Q10) of DON biodegradation

was significantly lower than that of DOC biodegradation. These results are supported by Schutt et al. (2014), who concluded that microorganisms prefer to mineralise N-rich organic substrates and the temperature sensitivity of N mineralisation is lower than that of C mineralisation. Additionally, natural vegetation restoration exerted a negligible effect on the temperature sensitivity of DON biodegradation, which was inconsistent with our hypothesis 3. The SEM 2 results indicated that the temperature sensitivity of the DON biodegradation was directly affected by the temperature sensitivity of enzyme activities involved in N and P cycling. Further, MBC played a vital role in regulating the temperature sensitivity of the DON biodegradation. It has been reported that the temperature sensitivity of N mineralisation is affected by soil total nitrogen, soil C:N ratio, and soil pH (Liu et al., 2016; Liu et al., 2017b; Miller and Geisseler, 2018). Our results indicated that the temperature sensitivity of DON biodegradation was likely related to P cycling processes and microbial carbon availability.

DOP biodegradation significantly increased with increasing temperature after the 60-day incubation period (Fig. S4), which was in agreement with our hypothesis 2. However, this is in contrast to Andry et al. (2019) who reported that temperature exerted a negligible effect on the P-fixation process in Ferralsol due to high soil P sorption capacity. Factors affecting DOP biodegradation shifted from C2, gram-negative bacterial PLFA, MBP, and the fungi to bacteria ratio at 4 °C to MBP at 20 °C and MBN at 35 °C. Therefore, it is likely that protein-like substrates and microbial phosphorus availability limited DOP biodegradation at low temperatures while microbial nitrogen availability influenced DOP biodegradation at high temperatures. The temperature sensitivity of the DOP biodegradation significantly increased within the first 130 years of vegetation restoration, rapidly decreased between 130 and 160 y, and finally was as low as that at S0 (Fig. 4), which partly supported our hypothesis 3. The SEM 3 results indicated that the temperature sensitivity of the DOP biodegradation was directly affected by C4 concentrations, and the temperature sensitivity of enzyme activities involved in N and P cycling which was directly affected by soil fungi. Therefore, the low temperature sensitivity of the DOP biodegradation rate at S160 was affected by the significantly decreased concentrations of C4 and soil fungi (130~160 y) and the low temperature sensitivity of NAG and AP activities (S160).

5. Conclusions

This study comprehensively investigated the effects of natural vegetation restoration and temperature on DOM biodegradation in the Ziwuling forest region of the Loess Plateau, China. DOC biodegradation significantly decreased in response to natural vegetation restoration. Further, farmland abandonment significantly decreased the biodegradation of DON and DOP. Generally, an increase in temperature significantly promoted the biodegradation of DOC, DON, and DOP by enhancing the microbial utilisation efficiencies of recalcitrant humic substrates (i.e., low-molecular-weight humic materials). Significantly decreased concentrations of C1 and C4 from 130 to 160 y, increased microbial PLFA (i.e., gram-negative bacteria, fungi, and AMF) from 100 to 160 y, and low temperature sensitivities of NAG and AP activities contributed to the low temperature sensitivities of the DOC and DOP biodegradation rates at the climax forest stage. However, natural vegetation restoration exerted a negligible effect on the temperature sensitivity of the DON biodegradation rate. Our results suggest that DOM biodegradability and the temperature sensitivity of DOM biodegradation were regulated by interactions between the biodegradation processes of DOC, DON, and DOP. Natural vegetation restoration could prevent DOM biodegradation, thus increasing the bioavailable organic matter in the Loess Plateau soils. Specifically, pioneer (*Populus davidiana*) and mingled (*Populus davidiana* and *Quercus liaotungensis*) forest stages were important for the recovery and accumulation of soil DON and DOP, respectively. Further, the climax forest community (*Quercus liaotungensis*) played a vital role in reducing DOC and DOP losses due to reduced temperature sensitivity of biodegradation.

Declaration of Competing Interest

The authors declare that they have no known competing financial interests or personal relationships that could have appeared to influence the work reported in this paper.

Acknowledgements

We thank the anonymous editors and reviewers for suggestions on the manuscript. Funding for this research came from National Key Research and Development Program of China (2016YFC0501707), and National Natural Science Foundation of China (41771557).

Supplementary materials

Supplementary material associated with this article can be found, in the online version, at doi:10.1016/j.watres.2020.116792.

References

A'Bear, A.D., Jones, T.H., Kandeler, E., Boddy, L, 2014. Interactive effects of temperature and soil moisture on fungal-mediated wood decomposition and extracellular enzyme activity. Soil Biol. Biochem. 70, 151–158.
Ali, R.S., Ingwersen, J., Demyan, M.S., Funkuin, Y.N., Wizemann, H.-D., Kandeler, E., Poll, C., 2015. Modelling in situ activities of enzymes as a tool to explain seasonal variation of soil respiration from agro-ecosystems. Soil Biol. Biochem. 81, 291–303.
Allison, S.D., Wallenstein, M.D., Bradford, M.A., 2010. Soil-carbon response to warming dependent on microbial physiology. Nat. Geosci. 3 (5), 336–340.
Andry, A., Tiphaine, C., Dominique, M., Herintsitohaina, R., Tantely, R., 2019. Land management modifies the temperature sensitivity of soil organic carbon, nitrogen and phosphorus dynamics in a Ferralsol. Appl. Soil Ecol. 138, 112–122.
Blagodatskaya, E., Kuzyakov, Y., 2008. Mechanisms of real and apparent priming effects and their dependence on soil microbial biomass and community structure: critical review. Biol. Fertil. Soils 45 (2), 115–131.
Chen, C., 1954. The vegetation and its roles in soil and water conservation in the secondary forest area in the boundary of Shaanxi and Gansu provinces. Acta Phytoecol. Geobot. Sin. 2, 152–153.
Chen, W., Westerhoff, P., Leenheer, J.A., Booksh, K., 2003. Fluorescence excitation−emission matrix regional integration to quantify spectra for dissolved organic matter. Environ. Sci. Technol. 37 (24), 5701–5710.
Cheng, L., Booker, F.L., Tu, C., Burkey, K.O., Zhou, L.S., Shew, H.D., Rufty, T.W., Hu, S.J., 2012. Arbuscular mycorrhizal fungi increase organic carbon decomposition under elevated CO_2. Science 337 (6098), 1084–1087.
Conant, R.T., Ryan, M.G., Ågren, G.I., Birge, H.E., Davidson, E.A., Eliasson, P.E., Evans, S.E., Frey, S.D., Giardina, C.P., Hopkins, F.M., Hyvönen, R., Kirschbaum, M.U.F., Lavallee, J.M., Leifeld, J., Parton, W.J., Megan Steinweg, J., Wallenstein, M.D., Martin Wetterstedt, Bradford, M.A., 2011. Temperature and soil organic matter decomposition rates – synthesis of current knowledge and a way forward. Global Change Biol. 17 (11), 3392–3404.
Cory, R.M., McKnight, D.M., 2005. Fluorescence spectroscopy reveals ubiquitous presence of oxidized and reduced quinones in dissolved organic matter. Environ. Sci. Technol. 39 (21), 8142–8149.
Davidson, E.A., Janssens, I.A., Luo, Y., 2006. On the variability of respiration in terrestrial ecosystems: moving beyond Q10. Global Change Biol. 12 (2), 154–164.
Deng, L., Wang, K., Tang, Z., Shangguan, Z., 2016. Soil organic carbon dynamics following natural vegetation restoration: Evidence from stable carbon isotopes (delta C-13). Agric. Ecosyst. Environ. 221, 235–244.
Doyle, A., Weintraub, M.N., Schimel, J.P., 2004. –. Soil Sci. Soc. Am. J. 68 (2), 669–676.
Fellman, J.B., D'Amore, D.V., Hood, E., Boone, R.D., 2008. Fluorescence characteristics and biodegradability of dissolved organic matter in forest and wetland soils from coastal temperate watersheds in southeast Alaska. Biogeochemistry 88 (2), 169–184.
Fontaine, S., Mariotti, A., Abbadie, L., 2003. The priming effect of organic matter: a question of microbial competition? Soil Biol. Biochem. 35 (6), 837–843.
Frey, S.D., Lee, J., Melillo, J.M., Six, J., 2013. The temperature response of soil microbial efficiency and its feedback to climate. Nat. Climate Change 3 (4), 395–398.
Galhardo, C.X., Masini, J.C., 2000. Spectrophotometric determination of phosphate and silicate by sequential injection using molybdenum blue chemistry. Anal. Chim. Acta 417 (2), 191–200.

German, D.P., Marcelo, K.R.B., Stone, M.M., Allison, S.D, 2012. The Michaelis–Menten kinetics of soil extracellular enzymes in response to temperature: a cross-latitudinal study. Glob. Change Biol. 18 (4), 1468–1479.
Ghani, A., Sarathchandra, U., Ledgard, S., Dexter, M., Lindsey, S., 2013. Microbial decomposition of leached or extracted dissolved organic carbon and nitrogen from pasture soils. Biol. Fertil. Soils 49 (6), 747–755.
Goberna, M., Garcia, C., Insam, H., Hernandez, M., Verdu, M., 2012. Burning fire-prone mediterranean shrublands: immediate changes in soil microbial community structure and ecosystem functions. Microb. Ecol. 64 (1), 242–255.
Huang, W., McDowell, W.H., Zou, X., Ruan, H., Wang, J., Ma, Z., 2015. Qualitative differences in headwater stream dissolved organic matter and riparian water-extractable soil organic matter under four different vegetation types along an altitudinal gradient in the Wuyi Mountains of China. Appl. Geochem. 52, 67–75.
Kaiser, K., Kalbitz, K., 2012. Cycling downwards – dissolved organic matter in soils. Soil Biol. Biochem. 52, 29–32.
Kalbitz, K., Schmerwitz, J., Schwesig, D., Matzner, E., 2003a. Biodegradation of soil-derived dissolved organic matter as related to its properties. Geoderma 113 (3-4), 273–291.
Kalbitz, K., Schmerwitz, J., Schwesig, D., Matzner, E., 2003b. Biodegradation of soil-derived dissolved organic matter as related to its properties. Geoderma 113 (3), 273–291.
Kalbitz, K., Solinger, S., Park, J.H., Michalzik, B., Matzner, E., 2000. Controls on the dynamics of dissolved organic matter in soils: a review. Soil Sci. 165 (4), 277–304.
Kisand, V., Rocker, D., Simon, M., 2008. Significant decomposition of riverine humic-rich DOC by marine but not estuarine bacteria assessed in sequential chemostat experiments. Aquat. Microb. Ecol. 53 (2), 151–160.
Liu, H.F., Wu, Y., Ai, Z.M., Zhang, J.Y., Zhang, C., Xue, S., Liu, G.B., 2019. Effects of the interaction between temperature and revegetation on the microbial degradation of soil dissolved organic matter (DOM) - a DOM incubation experiment. Geoderma 337, 812–824.
Liu, Y., He, N.P., Wen, X.F., Yu, G.R., Gao, Y., Jia, Y.L., 2016. Patterns and regulating mechanisms of soil nitrogen mineralization and temperature sensitivity in Chinese terrestrial ecosystems. Agric. Ecosyst. Environ. 215, 40–46.
Liu, Y., He, N.P., Zhu, J.X., Xu, L., Yu, G.R., Niu, S.L., Sun, X.M., Wen, X.F., 2017a. Regional variation in the temperature sensitivity of soil organic matter decomposition in China's forests and grasslands. Glob. Change Biol. 23 (8), 3393–3402.
Liu, Y., Wang, C.H., He, N.P., Wen, X.F., Gao, Y., Li, S.G., Niu, S.L., Butterbach-Bahl, K., Luo, Y.Q., Yu, G.R., 2017b. A global synthesis of the rate and temperature sensitivity of soil nitrogen mineralization: latitudinal patterns and mechanisms. Glob. Change Biol. 23 (1), 455–464.
Lu, Y., Wassmann, R., Neue, H.-U., Huang, C., 2000. Dynamics of Dissolved Organic Carbon and Methane Emissions in a Flooded Rice Soil. Soil Sci. Soc. Am. J. 64 (6), 2011–2017.
Luo, Z., Wang, E., Sun, O.J., 2016. A meta-analysis of the temporal dynamics of priming soil carbon decomposition by fresh carbon inputs across ecosystems. Soil Biol. Biochem. 101, 96–103.
Ma, Y., McCormick, M.K., Szlavecz, K., Filley, T.R., 2019. Controls on soil organic carbon stability and temperature sensitivity with increased aboveground litter input in deciduous forests of different forest ages. Soil Biol. Biochem. 134, 90–99.
Mao, R., Li, S.-Y., 2018. Temperature sensitivity of biodegradable dissolved organic carbon increases with elevating humification degree in subtropical rivers. Sci. Total Environ. 635, 1367–1371.
Marschner, B., Kalbitz, K., 2003. Controls of bioavailability and biodegradability of dissolved organic matter in soils. Geoderma 113 (3), 211–235.
McDowell, W.H., Zsolnay, A., Aitkenhead-Peterson, J.A., Gregorich, E.G., Jones, D.L., Jödemann, D., Kalbitz, K., Marschner, B., Schwesig, D, 2006. A comparison of methods to determine the biodegradable dissolved organic carbon from different terrestrial sources. Soil Biol. Biochem. 38 (7), 1933–1942.
Miller, K.S., Geisseler, D, 2018. Temperature sensitivity of nitrogen mineralization in agricultural soils. Biol. Fertil. Soils 54 (7), 853–860.
Min, K., Buckeridge, K., Ziegler, S.E., Edwards, K.A., Bagchi, S., Billings, S.A., 2019. Temperature sensitivity of biomass-specific microbial exo-enzyme activities and CO_2 efflux is resistant to change across short- and long-term timescales. Glob. Change Biol. 25 (5), 1793–1807.
Morrison, E., Lagos, L., Al-Agely, A., Glaab, H., Johnson, W., Jorquera, M.A., Ogram, A., 2017. Mycorrhizal inoculation increases genes associated with nitrification and improved nutrient retention in soil. Biol. Fertil. Soils 53 (3), 275–279.
Müller, K., Kramer, S., Haslwimmer, H., Marhan, S., Scheunemann, N., Butenschön, O., Scheu, S., Kandeler, E., 2016. Carbon transfer from maize roots and litter into bacteria and fungi depends on soil depth and time. Soil Biol. Biochem. 93, 79–89.
Murphy, J., Riley, J.P., 1962. A modified single solution method for the determination of phosphate in natural waters. Anal. Chim. Acta 27, 31–36.
Murphy, K.R., Ruiz, G.M., Dunsmuir, W.T.M., Waite, T.D, 2006. Optimized parameters for fluorescence-based verification of ballast water exchange by ships. Environ. Sci. Technol. 40 (7), 2357–2362.
Nazaries, L., Tottey, W., Robinson, L., Khachane, A., Abu Al-Soud, W., Sorensen, S., Singh, B.K., 2015. Shifts in the microbial community structure explain the response of soil respiration to land-use change but not to climate warming. Soil Biol. Biochem. 89, 123–134.
Ohno, T., 2002. Fluorescence inner-filtering correction for determining the humification index of dissolved organic matter. Environ. Sci. Technol. 36 (4), 742–746.
Ortiz-Álvarez, R., Fierer, N., de los Ríos, A., Casamayor, E.O., Barberán, A., 2018. Consistent changes in the taxonomic structure and functional attributes of bacterial communities during primary succession. ISME J. 12 (7), 1658–1667.
Pang, X.Y., Zhu, B.A., Lu, X.T., Cheng, W.X., 2015. Labile substrate availability controls temperature sensitivity of organic carbon decomposition at different soil depths. Biogeochemistry 126 (1-2), 85–98.
Paul, E.A., Clark, F.E., 1996. Soil Microbiology and Biochemistry. Academic Press, San Diego.
Peay, K.G., Kennedy, P.G., Bruns, T.D., 2008. Fungal Community ecology: a hybrid beast with a molecular master. Bioscience 58 (9), 799–810.
Prach, K., Walker, L.R., 2011. Four opportunities for studies of ecological succession. Trends Ecol. Evol. 26 (3), 119–123.
Schmidt, S.K., Cleveland, C.C., Nemergut, D.R., Reed, S.C., King, A.J., Sowell, P., 2011. Estimating phosphorus availability for microbial growth in an emerging landscape. Geoderma 163 (1), 135–140.
Schutt, M., Borken, W., Spott, O., Stange, C.F., Matzner, E., 2014. Temperature sensitivity of C and N mineralization in temperate forest soils at low temperatures. Soil Biol. Biochem. 69, 320–327.
Stedmon, C.A., Bro, R., 2008. Characterizing dissolved organic matter fluorescence with parallel factor analysis: a tutorial. Limnol. Oceanography: Methods 6 (11), 572–579.
Stedmon, C.A., Markager, S., 2005. Resolving the variability in dissolved organic matter fluorescence in a temperate estuary and its catchment using PARAFAC analysis. Limnol. Oceanogr. 50 (2), 686–697.
Stedmon, C.A., Markager, S., Bro, R., 2003. Tracing dissolved organic matter in aquatic environments using a new approach to fluorescence spectroscopy. Mar. Chem. 82 (3), 239–254.
Teutscherova, N., Vazquez, E., Arango, J., Arevalo, A., Benito, M., Pulleman, M., 2019. Native arbuscular mycorrhizal fungi increase the abundance of ammonia-oxidizing bacteria, but suppress nitrous oxide emissions shortly after urea application. Geoderma 338, 493–501.
van Hees, P.A.W., Jones, D.L., Finlay, R., Godbold, D.L., Lundström, U.S., 2005. The carbon we do not see—the impact of low molecular weight compounds on carbon dynamics and respiration in forest soils: a review. Soil Biol. Biochem. 37 (1), 1–13.
von Lützow, M., Kögel-Knabner, I., 2009. Temperature sensitivity of soil organic matter decomposition—what do we know? Biol. Fertil. Soils 46 (1), 1–15.
Wang, J., Liu, G., Zhang, C., Wang, G., Fang, L., Cui, Y., 2019. Higher temporal turnover of soil fungi than bacteria during long-term secondary succession in a semiarid abandoned farmland. Soil Tillage Res. 194, 104305.
Wang, Q., Liu, S., Tian, P., 2018. Carbon quality and soil microbial property control the latitudinal pattern in temperature sensitivity of soil microbial respiration across Chinese forest ecosystems. Glob. Change Biol. 24 (7), 2841–2849.
Ylla, I., Romaní, A.M., Sabater, S., 2012. Labile and recalcitrant organic matter utilization by river biofilm under increasing water temperature. Microb. Ecol. 64 (3), 593–604.
Zhang, L., Shi, N., Fan, J., Wang, F., George, T.S., Feng, G., 2018. Arbuscular mycorrhizal fungi stimulate organic phosphate mobilization associated with changing bacterial community structure under field conditions. Environ. Microbiol. 20 (7), 2639–2651.
Zhang, L., Xu, M., Liu, Y., Zhang, F., Hodge, A., Feng, G., 2016. Carbon and phosphorus exchange may enable cooperation between an arbuscular mycorrhizal fungus and a phosphate-solubilizing bacterium. New Phytol. 210 (3), 1022–1032.
Zhong, Y., Yan, W., Wang, R., Wang, W., Shangguan, Z., 2018. Decreased occurrence of carbon cycle functions in microbial communities along with long-term secondary succession. Soil Biol. Biochem. 123, 207–217.
Zou, H.Y., Liu, G.B., Wang, H.S., 2002. The vegetation development in North Ziwuling forest region in last fifty years. Acta Bot. Boreali-Occidentalia Sin. 22, 1–8.